

Synthesis of dinuclear complexes of rhenium(I) as potential metallomesogens

Marie-Andrée Guillevis,^a Mark E. Light,^b Simon J. Coles,^b Thomas Gelbrich,^b Michael B. Hursthouse^b and Duncan W. Bruce^{*a}

^a School of Chemistry, University of Exeter, Stocker Road, Exeter, UK EX4 4QD.

E-mail: d.bruce@exeter.ac.uk

^b EPSRC Crystallographic Service, Department of Chemistry, University of Southampton, Highfield Road, Southampton, UK SO17 1BJ

Received 21st December 1999, Accepted 17th March 2000

Published on the Web 10th April 2000

Seven anisotropic diimines and their corresponding dinuclear complexes of rhenium(I) have been synthesized. The crystal and molecular structures of one of the diimines and two of the complexes were determined. In common with related imine ligands which have been synthesized previously, the new diimines were mesomorphic showing smectic C and nematic phases and, in some cases, smectic I and crystal J phases. However, none of the orthometallated, dinuclear complexes showed any liquid crystal phases.

In the synthesis of materials of any kind¹ a major motivation is to be able to exert control over the properties in a predictable way, ideally *via* the initial synthesis. In the general field of liquid crystals this is quite a well developed art and so it is possible to influence physical properties such as birefringence and dielectric anisotropy.

The advent of widespread interest in metallomesogens in the mid-1980s provided an extra challenge in this regard as the co-ordination of suitable ligands to the metal centre provided an extra perturbation which needed to be understood. Metal centres introduce extra parameters into a liquid-crystalline system and it is necessary to worry about the effects of, for example, co-ordination geometry, electronic configuration and reactivity.²

As part of our studies in this area we have looked at the problem of incorporating six-co-ordinate metal centres into rod-like (calamitic) liquid crystals. Briefly stated, the potential problem is that liquid crystal mesophase formation requires molecules with a rather high structural anisotropy which in turn leads to anisotropic dispersion forces which stabilise the mesophase. Tethering rod-like ligands to a planar or linear metal centre (d^8 – d^{10}) is consistent with this requirement, but an octahedral centre can reduce the anisotropy and suppress mesophase formation.³

We succeeded in the realisation of calamitic liquid crystals containing six-co-ordinate metal centres initially using ortho-metallated imine complexes of Mn^{14,5} (Fig. 1) although we now study their rhenium(I) congeners for choice due to their higher thermal stability.^{6,7} We then reported examples of other calamitic systems using diazabutadienes⁸ and 2,2'-bipyridines as ligands to Re^{1,9}. One of the interesting features which a comparison of these series of materials revealed was that in the case of the imine complexes the liquid crystal transition temperatures of the ligand were reduced on complexation to the metal fragment ($\text{Re}(\text{CO})_4$), while for the main part they were maintained or increased for complexation of the metal fragment ($\text{ReBr}(\text{CO})_3$) to the diazabutadiene and bipyridine systems. This being the case, would it then also be true that if we were to introduce more than one $\text{Re}(\text{CO})_4$ fragment into the imine systems the transition temperatures would reduce even further? In order to attempt to answer this question we undertook the

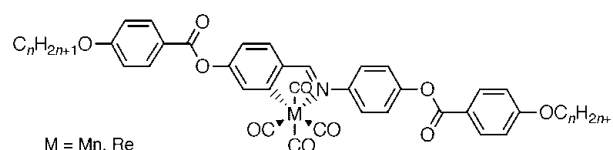


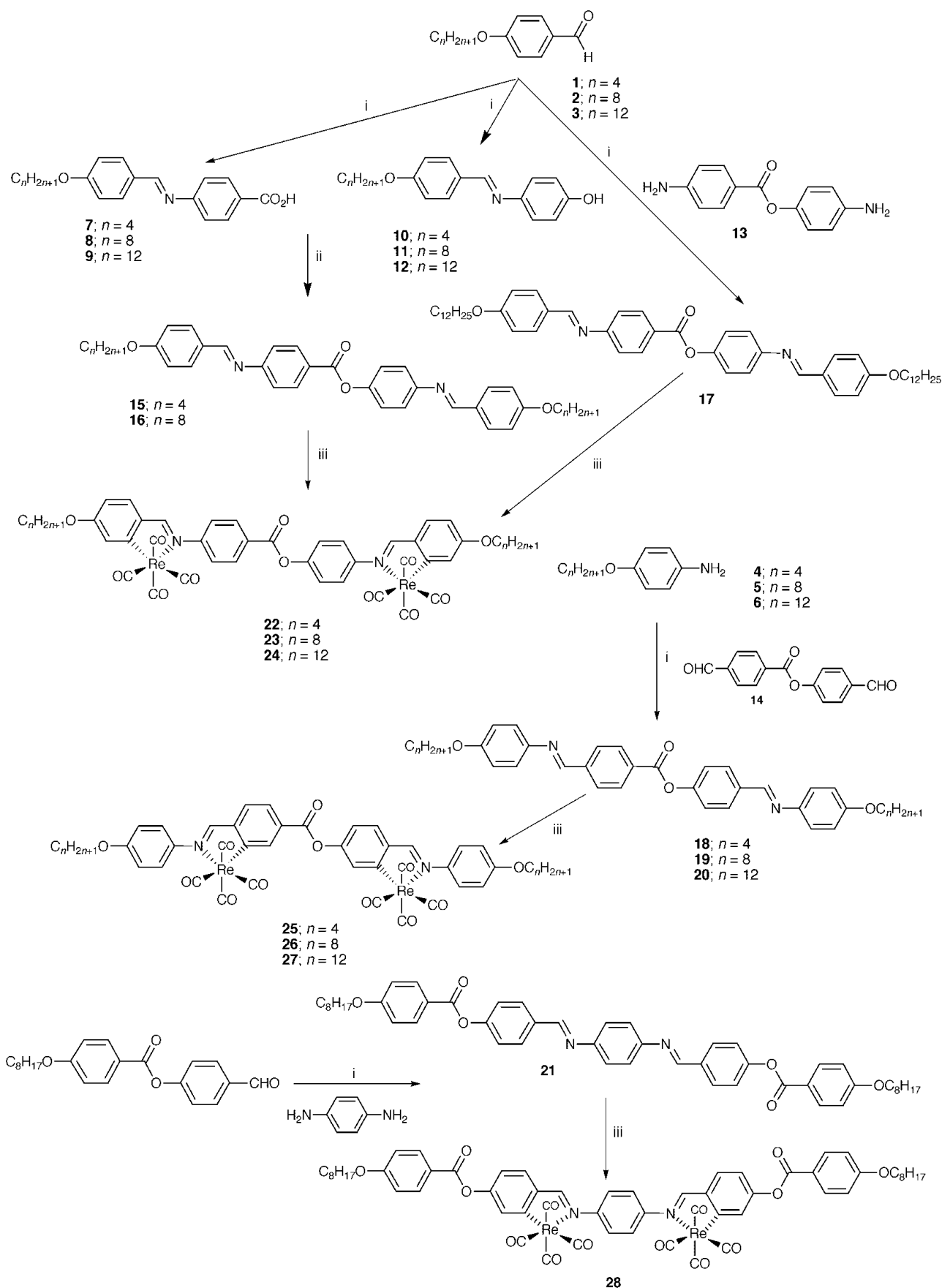
Fig. 1 Structure of some manganese and rhenium imine complexes studied previously.

synthesis of some ligands with two, isolated imine functions which would allow the co-ordination of two $\text{Re}(\text{CO})_4$ groups. The results of this study are now reported.

Results and discussion

Synthesis of the ligands and complexes

The synthetic routes are outlined in Scheme 1 and we note that related, unsubstituted 'ligands' have been reported previously by Miyajima and Matsunaga.¹⁰ Alkoxybenzaldehydes (**1–3**) were obtained *via* a Williamson ether reaction between the relevant 1-bromoalkane and 4-hydroxybenzaldehyde, while alkoxyanilines (**4–6**) were obtained by a reaction between a 1-bromoalkane and 4-acetamidophenol to give 4-alkoxyphenylacetamide, followed by deprotection to give the amine. The imines **7–12** were then obtained in yields of 70–80% by reaction of the benzaldehyde with a relevant amine in a Schiff base condensation and two target, symmetric diimines (**15** and **16**) were then produced in yields of around 80% by esterification of the carboxylic acids **7**, **8** with the phenols **10**, **11** using DCC/DMAP [dicyclohexylcarbodiimide/4(*N,N*-dimethylamino)pyridine]. For reasons which we cannot fathom, diimine **17** could not be obtained in this way as the esterification failed and so it was obtained in 55% yield *via* direct reaction with the diamine **13** which would represent a preferred, more convergent future synthesis for symmetric diimines of this type. Finally, three isomeric diimines, **18–20**, were obtained in 80–100% yields by reaction of the alkoxyanilines **4–6** with the dialdehyde **14**. In addition, we synthesized one five-ring diimine, **21**. This was obtained by esterification of octyloxybenzoic acid with 4-hydroxybenzaldehyde to give 4-(4'-octyloxybenzoyloxy)benz-



Scheme 1 Synthesis of the ligands and complexes. (i) EtOH/H⁺, (ii) CH₂Cl₂/DCC/DMAP, (iii) [ReMe(CO)₅]/toluene/reflux.

aldehyde, two equivalents of which were then condensed with 1,4-phenylenediamine to give the target diimine.

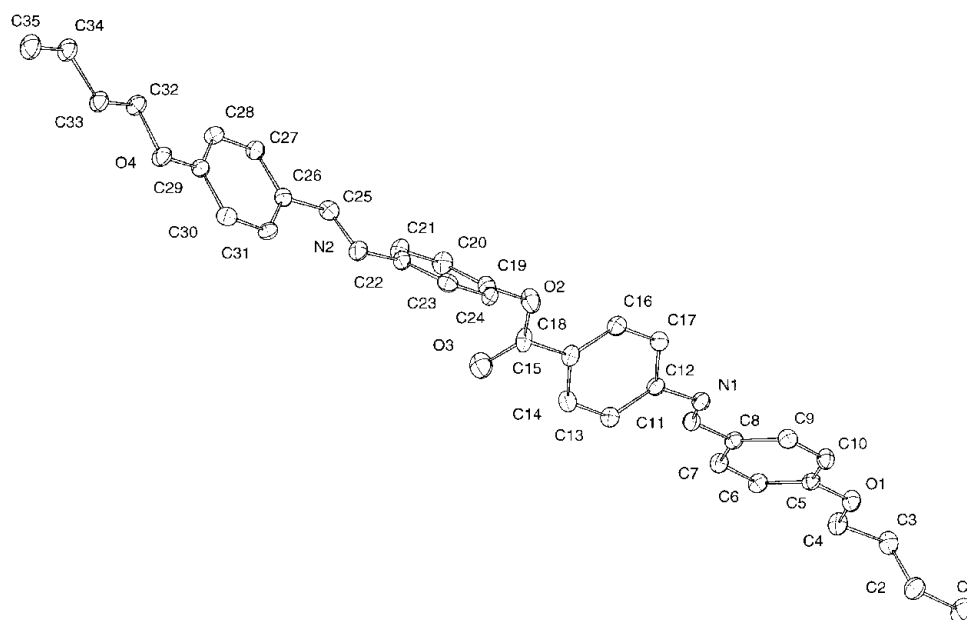
The related metal complexes (**22–28**) were finally obtained by reaction of the diimines with [ReMe(CO)₅] in toluene at reflux for 20 h.

All of the ligands and their complexes were characterised by ¹H and ¹³C NMR spectroscopy and, for the complexes, infrared spectroscopy which showed ν_{CO} at 2090, 1988 and 1922 cm⁻¹.¹¹

It is worthy of note that in the course of this work we tried a variety of methods to obtain the related monometallated

Table 1 Crystallographic data for compounds **15**, **22** and **26**

	15	22	26
Formula	C ₃₅ H ₃₆ N ₂ O ₄	C ₄₃ H ₃₄ N ₂ O ₁₂ Re ₂	C ₅₁ H ₅₀ N ₂ O ₁₂ Re ₂
<i>M</i>	548.66	1143.12	1255.33
Crystal system	Triclinic	Triclinic	Triclinic
Space group	<i>P</i> $\bar{1}$	<i>P</i> $\bar{1}$	<i>P</i> $\bar{1}$
<i>a</i> /Å	7.2025(6)	8.5056(2)	9.1822(2)
<i>b</i> /Å	10.1729(13)	11.9274(3)	13.527(3)
<i>c</i> /Å	20.231(3)	21.6445(8)	21.470(4)
α /°	83.619(5)	82.0034(19)	74.14(3)
β /°	87.892(8)	82.2317(18)	86.93(3)
γ /°	83.518(8)	71.9589(18)	74.32(3)
<i>U</i> /Å ³	1463.3(3)	2057.66(10)	2469.1(9)
<i>T</i> /K	150(2)	150(2)	150(2)
<i>Z</i>	2	2	2
μ /mm ⁻¹	0.081	5.943	4.961
No. reflections measured	2.0691	28995	46405
No. unique reflections	5576	7333	25880
<i>R</i> 1 [<i>I</i> > 2 σ (<i>I</i>)]	0.0782	0.0367	0.0372
<i>wR</i> 2 [<i>I</i> > 2 σ (<i>I</i>)]	0.2201	0.0898	0.0895

**Fig. 2** Molecular structure of ligand **15**.

derivatives of ligands **15–20** by using half-stoichiometric amounts of [ReMe(CO)₅] and by varying reaction conditions. However, while we obtained spectroscopic evidence that the complex formed, it proved impossible to isolate a pure sample.

Crystal and molecular structure of compounds **15**, **22** and **26**

In order to try to obtain as much information as possible on these new materials, single crystal structure determinations were carried out on ligand **15** and complexes **22** and **26** for which we were able to grow suitable crystals.

Ligand 15. Crystals suitable for diffraction studies were grown from dichloromethane/hexane. The molecules crystallised in a triclinic lattice in space group *P* $\bar{1}$ and after refinement an *R* factor of just under 8% was achieved. Crystallographic parameters are collected in Table 1, selected bond lengths, angles and least squares mean plane torsion angles in Table 2 and the molecular structure is shown in Fig. 2.

The angles between the least squares planes of the four rings are not restricted by any chemical constraints and are thus a feature of the packing arrangement. C5 > C10–C12 > C17 39.81(4), C12 > C17–C19 > C24 76.79(10) and C19 > C24–C26 > C31 38.68(13)°. The largest angle is between the rings

joined by the ester group which approaches the stereochemically favoured 90°. The angles between the 1st and 2nd and 3rd and 4th rings across the imine double bond are rather similar to each other.

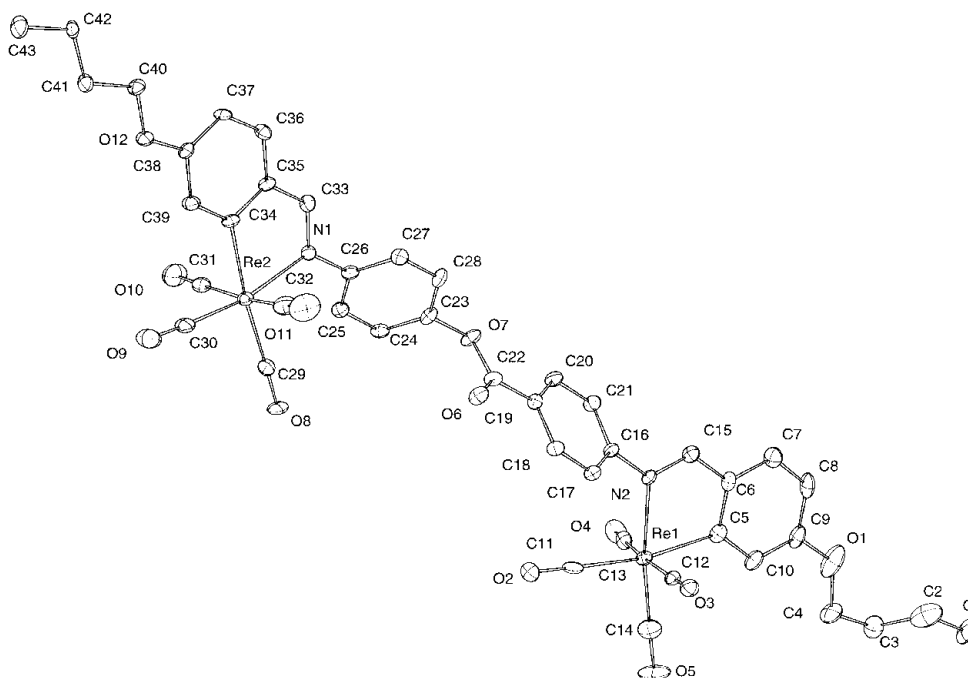
The molecules within the crystal stack parallel along the *a* direction and antiparallel along the *b* direction. The terminal chain contains a *gauche* bond at one end while all those at the other are *trans*, which may be due to packing effects optimising the possibility for the interdigitation of alternate chains.

Complex 22. Crystals suitable for diffraction studies were grown from dichloromethane/hexane. The molecules crystallised in a triclinic lattice in space group *P* $\bar{1}$ and after refinement an *R* factor of 3.7% was achieved. The chain at one end of the molecule was modelled as disordered over two conformations. The molecular structure is shown in Fig. 3.

The co-ordination of the metal tetracarbonyl group has increased the angle between pairs of adjacent rings. The angles between the least square planes of the four rings are C5 > C10–C16 > C21 47.93(21), C16 > C21–C23 > C28 84.24(17) and C23 > C28–C34 > C39 42.55(21)°. This can simply be attributed to the steric demands of the metal carbonyl functions (as shown in the space-filling model in Fig. 4) which twist the ester-bridged rings further apart, each nestled between two carbonyl

Table 2 Selected bond lengths (Å) and angles (°) and least squares mean plane torsion angles (°) for compounds **15**, **22** and **26**

		Complex 26			
Complex 22		Molecule 1		Molecule 2	
Re(1)–C(14)	1.924(7)	Re(1)–C(17)	1.92(3)	Re(3)–C(69)	1.92(2)
Re(1)–C(11)	1.963(7)	Re(1)–C(15)	1.98(2)	Re(3)–C(70)	1.96(3)
Re(1)–C(13)	1.980(6)	Re(1)–C(16)	1.98(2)	Re(3)–C(68)	1.98(3)
Re(1)–C(12)	2.000(6)	Re(1)–C(18)	1.99(3)	Re(3)–C(67)	2.02(3)
Re(2)–C(30)	1.921(7)	Re(2)–C(35)	1.93(2)	Re(4)–C(87)	1.90(2)
Re(2)–C(29)	1.973(7)	Re(2)–C(36)	1.95(2)	Re(4)–C(89)	1.97(2)
Re(2)–C(31)	1.980(7)	Re(2)–C(37)	1.97(3)	Re(4)–C(88)	1.97(2)
Re(2)–C(32)	1.981(7)	Re(2)–C(34)	2.00(3)	Re(4)–C(86)	1.99(2)
C(14)–Re(1)–C(11)	91.8(3)	C(17)–Re(1)–C(15)	89.2(11)	C(69)–Re(3)–C(70)	85.9(9)
C(14)–Re(1)–C(13)	89.1(3)	C(17)–Re(1)–C(16)	92.6(10)	C(69)–Re(3)–C(68)	95.0(10)
C(11)–Re(1)–C(13)	93.2(2)	C(15)–Re(1)–C(16)	93.1(9)	C(70)–Re(3)–C(68)	91.5(11)
C(14)–Re(1)–C(12)	88.6(3)	C(17)–Re(1)–C(18)	86.5(11)	C(69)–Re(3)–C(67)	87.7(9)
C(11)–Re(1)–C(12)	93.2(2)	C(16)–Re(1)–C(18)	90.5(9)	C(68)–Re(3)–C(67)	90.2(10)
C(30)–Re(2)–C(29)	92.3(3)	C(35)–Re(2)–C(36)	93.6(9)	C(87)–Re(4)–C(89)	93.2(9)
C(30)–Re(2)–C(31)	87.8(3)	C(35)–Re(2)–C(37)	90.3(9)	C(87)–Re(4)–C(88)	89.2(10)
C(29)–Re(2)–C(31)	93.8(3)	C(36)–Re(2)–C(37)	90.7(10)	C(89)–Re(4)–C(88)	93.4(9)
C(30)–Re(2)–C(32)	89.9(3)	C(35)–Re(2)–C(34)	85.3(9)	C(87)–Re(4)–C(86)	88.6(10)
C(29)–Re(2)–C(32)	93.1(3)	C(36)–Re(2)–C(34)	92.3(10)	C(89)–Re(4)–C(86)	90.1(8)
O(2)–C(11)–Re(1)	176.6(5)	O(2)–C(15)–Re(1)	177.9(16)	O(14)–C(67)–Re(3)	176.5(18)
O(3)–C(12)–Re(1)	178.5(5)	O(3)–C(16)–Re(1)	176.8(19)	O(15)–C(68)–Re(3)	178(2)
O(4)–C(13)–Re(1)	175.0(6)	O(4)–C(17)–Re(1)	176(2)	O(16)–C(69)–Re(3)	174(2)
O(5)–C(14)–Re(1)	177.8(7)	O(5)–C(18)–Re(1)	178(2)	O(17)–C(70)–Re(3)	174.0(17)
O(8)–C(29)–Re(2)	177.4(5)	O(8)–C(34)–Re(2)	174.9(18)	O(20)–C(86)–Re(4)	175.2(17)
O(9)–C(30)–Re(2)	176.7(6)	O(9)–C(35)–Re(2)	175(2)	O(21)–C(87)–Re(4)	178.8(19)
O(10)–C(31)–Re(2)	176.8(6)	O(10)–C(36)–Re(2)	179.2(17)	O(22)–C(88)–Re(4)	176(2)
O(11)–C(32)–Re(2)	175.2(7)	O(11)–C(37)–Re(2)	175.8(16)	O(23)–C(89)–Re(4)	176.9(16)
(C5 > C10)–(C16 > C21)	47.93(21)	(C9 > C14)–(C20 > C25)	35.21(3)	(C90 > C95)–(C79 > C84)	35.73(4)
C16 > C21)–(C23 > C28)	84.24(17)	(C20 > C25)–(C27 > C32)	26.25(2)	(C79 > C84)–(C72 > C77)	24.47(3)
C23 > C28)–(C34 > C39)	42.55(21)	(C27 > C32)–(C38 > C66)	51.11(6)	(C72 > C77)–(C61 > C66)	48.85(5)
Ligand 15		(C12 > C17)–(C19 > C24)		(C19 > C24)–(C26 > C31)	38.68(13)
(C5 > C10)–(C12 > C17)	39.81(4)				

**Fig. 3** Molecular structure of complex **22**.

groups on opposing sides of the metal–metal axis. In comparison with the rhenium tetracarbonyl complex of benzylideneaniline,¹² the angle between the two rings is smaller due to the packing arrangement adopted. The molecules pack in essentially the same way as the parent ligand (**15**), namely paral-

lel along *a* and antiparallel along *b*. While the co-ordination of both metal centres on the same side of the molecule would seem energetically unfavourable, the molecules pack back-to-back such that the metal tetracarbonyl groups interlock, thus forming a stable packing arrangement (Fig. 5).

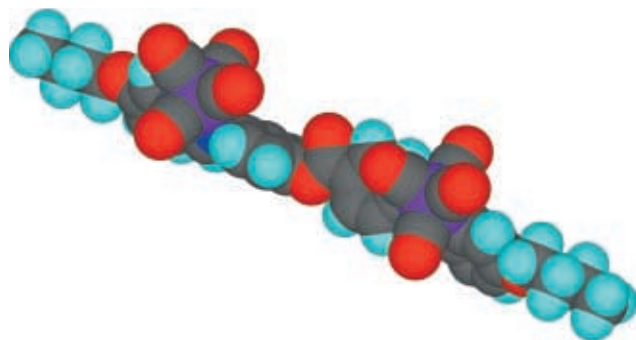


Fig. 4 Space-filling model of complex **22** to show the steric influence of the $\text{Re}(\text{CO})_4$ group.

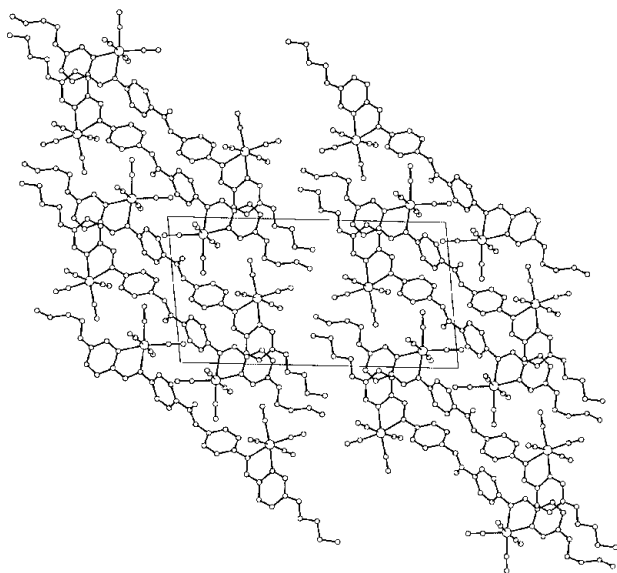


Fig. 5 Packing diagram for complex **22** viewed down the b axis (hydrogen atoms omitted for clarity).

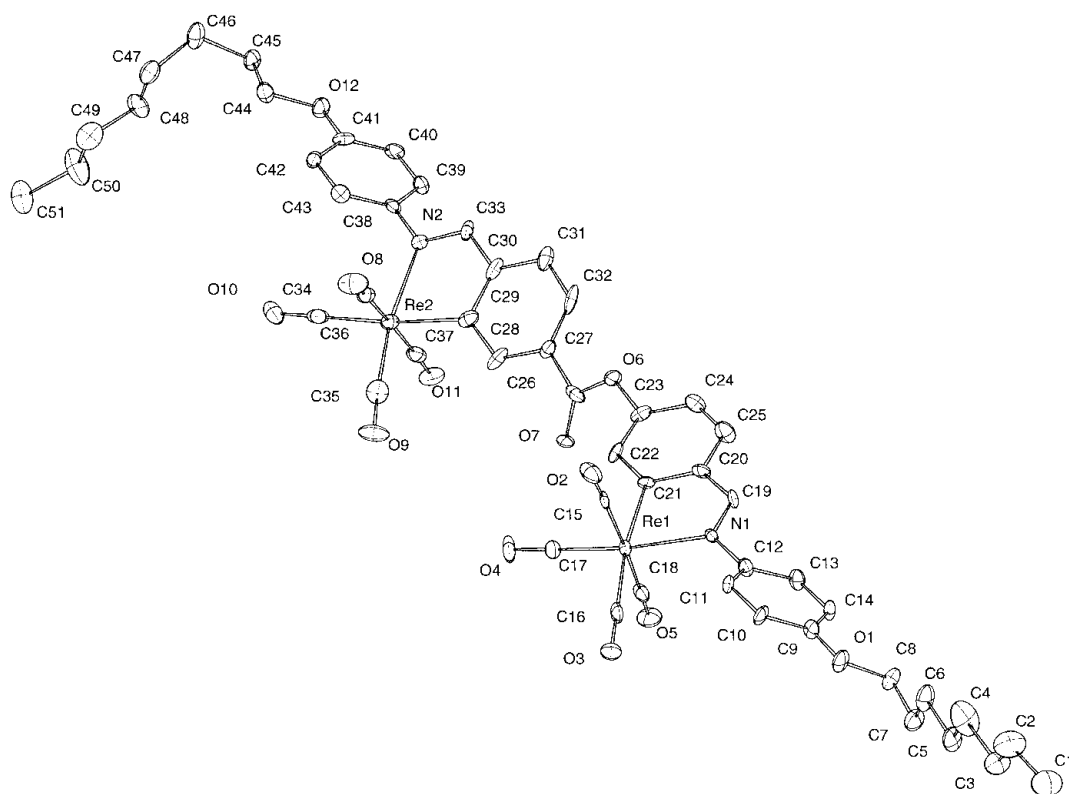


Fig. 6 Molecular structure of complex **26**.

The Re–C bond lengths are Re–C–O angles are comparable with those usually observed. The C–Re–C angles show slight deviation from the ideal 90° as might be expected due to steric hindrance of the phenyl ring.

Complex 26. Crystals suitable for diffraction studies were grown from dichloromethane/hexane. The molecules crystallised in a triclinic lattice in the non-centrosymmetric space group $P1$ and after refinement an R factor of 3.7% was achieved. The molecular structure is shown in Fig. 6.

Although the two molecules in the asymmetric unit appear to be related by an inversion centre, this symmetry is broken by two atoms. Thus, O7 and O18, the ester oxygens, deviate significantly from the centrosymmetric model. A refinement was tried in $P\bar{1}$ but the R values were higher than in the non-centrosymmetric space group, and the ester oxygens had large, elongated ellipsoids. However this difference is very small and can be ignored in comparison of the packing to that in complex **22**.

As with complex **22** the presence of the two Re atoms on the same side of the molecule is due to the interleaving way the molecules pack within the unit cell. However, the increased chain length would appear to have led to greater packing effects. Thus, the torsion angle between the least square planes of the ester-bridged rings which is $84.24(17)^\circ$ in **22** has closed up to $26.25(2)$ (molecule 1), $24.47(3)^\circ$ (molecule 2), causing more strain in the central part of the molecule, and resulting in the ester group adopting two slightly different conformations which is the origin of the two independent molecules in the asymmetric unit. The torsion angles between the least square planes of the 1st and 2nd and 3rd and 4th rings in the two independent molecules are $35.21(3)$, $35.73(4)$ and $51.11(6)$, $48.85(5)^\circ$, respectively. In contrast to **15** and **22**, these are very different and this fact arises from the longer chain length having an increased effect on the mode of packing. All the compounds show differences in the conformation of the end chains and this is exaggerated in the longer chain molecule, **26**.

The Re–C bond lengths and the Re–C–O angles show values within the expected range. However the increased steric strain (two central rings are close to parallel) causes higher distortion

Table 3 Thermal data for the new ligands and complexes

Compound	Transition	$T/^\circ\text{C}$	$\Delta H/\text{kJ mol}^{-1}$	$\Delta S/\text{J K}^{-1} \text{mol}^{-1}$
Diimines				
15	Crys–J	133	12.5	30.8
	J–N	155	32.4	75
	N–I (decomp.)	360	—	—
16	Crys–J	119	28.5	72
	J–S _c	129	5.6	14
	S _c –N	235	2.3	4
	N–I(decomp.)	325	0.7	1
17	Crys–S _I	111	72.3	185
	(J–S _I)	(110)	(22.2)	(61)
	S _I –S _c	124	3.5	9
	S _c –N	257	5.2	10
	N–I(decomp.)	280	1.8	3
18	Crys–S _c	196	48.6	104
	S _c –N	269	—	—
19	N–I(decomp.)	394	0.4	0
	Crys–Crys'	115	10.4	26
	Crys'–S _c	150	42.8	100
	S _c –N	314	0.1	0
20	N–I(decomp.)	334	2.5	4
	Crys–S _c	138	54.7	132
	(S _I –S _c)	(137)	(4.2)	(10)
	S _c –N	284	1.5	3
21	N–I(decomp.)	294	2.5	4
	Crys–Crys'	88	14.2	39
	Crys'–Crys''	117	8.2	21
	Crys''–J	144	8.6	20
	J–S _I	151	26.9	63
	S _I –S _c	167	0.7	2
	^a	172	1.8	4
	S _c –N	290	1.4	3
	N–I(decomp.)	422	—	—
Dirhenium complexes				
22	Crys–I(decomp.)	220	45.2	86
23	Crys–I(decomp.)	216	63.4	128
24	Crys–I	196	72.9	155
25	Crys–I(decomp.)	238	62.4	118
26	Crys–I	176	69.5	154
27	Crys–Crys'	128	6.4	16
28	Crys'–I	148	45.9	109
	Crys'–I	220	—	—

^a See the text for a discussion of this event.

of both Re–C–O angles and O≡C–Re–C≡O angles which range from 85.3(9) to 95.0(10)°.

Mesomorphism of the ligands

The mesomorphic properties of the diimines were obtained by polarising optical microscopy to obtain optical textures of the phases and differential scanning calorimetry (DSC) to evaluate the enthalpy change at phase transitions. Thermal data for the ligands are collected in Table 3.

All of the ligands showed a nematic phase (N) which was identified by its characteristic schlieren texture (Fig. 7) and highly fluid nature. Below the nematic phase each diimine, with the exception of **15**, also showed a smectic C phase which was identified on the basis of its characteristic texture (Fig. 8) and by the appearance of the familiar fingerprint texture at the smectic C-to-nematic transition (Fig. 9).¹³ Comparison of the transition temperatures shows that in **15**–**17**, as the terminal alkoxy chain is lengthened, the nematic phase is gradually destabilised (T_{NI} for **15** is 360 °C with decomposition, while for **17** it is 280 °C also with decomposition) while the smectic C phase is stabilised (not seen in **15**, but clearing at 257 °C in **17**). The same trend in nematic phase stability is also seen in diimines **18**–**20** although while the smectic C stability increases from **18** to **19**, it decreases at **20**. Further, ligands **15**–**17** also possess a crystal J phase (Fig. 10) the stability of which drops

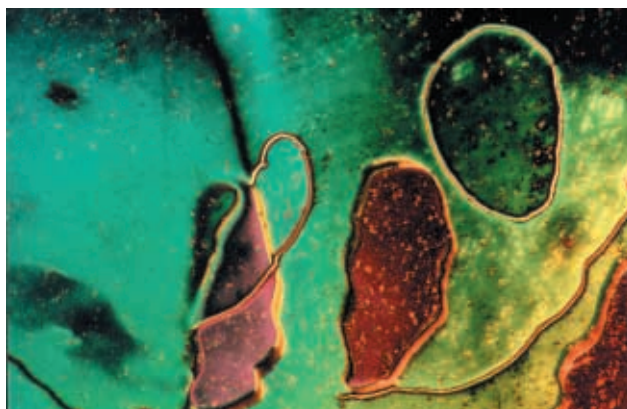


Fig. 7 The nematic phase of compound **16** on cooling at 298 °C.



Fig. 8 The transition between the nematic and smectic C phase of compound **16** at 236 °C on cooling showing the classic 'fingerprint' texture.

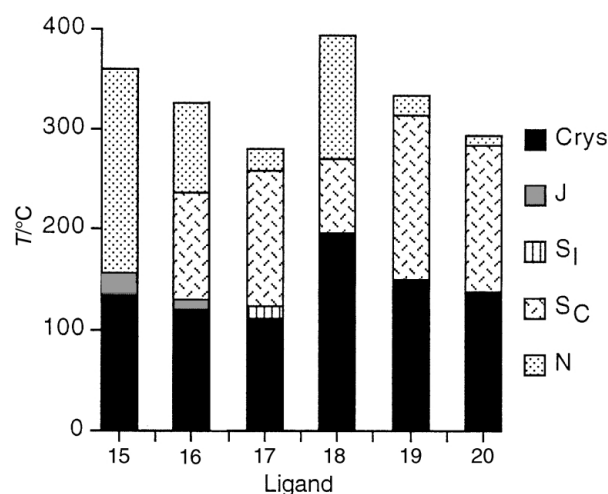


Fig. 9 Bar chart to show the mesomorphism of the ligands **15**–**20**.

from 155 °C in **15** to 110 °C in **17** where it is monotropic. The more anisotropic ligand, **21**, melted at 144 °C and showed a crystal smectic J phase, above which were smectic I and C phases and, eventually, a nematic phase with a range of over 130 °C; the ligand cleared with decomposition at 422 °C. The smectic I phase was identified both on account of the inability to focus well on the texture and the presence of a schlieren texture, both factors distinguishing it from the smectic F phase. Identification of the crystal J phase by microscopy was not unequivocal, but a J phase would be expected to follow a smectic I phase (with a crystal G phase following a smectic F). In addition, there is a direct analogy with related ligands where the identity of the crystal J phase was established by X-ray

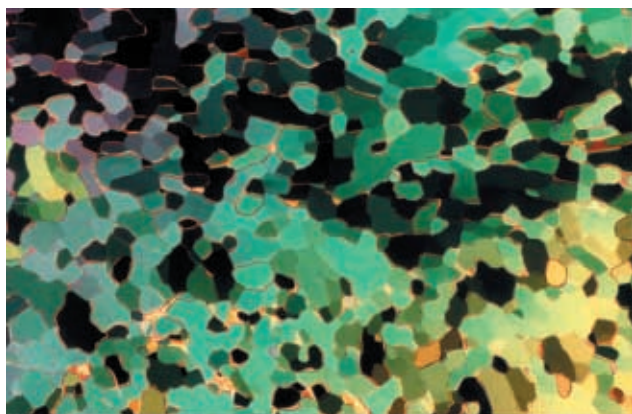


Fig. 10 Mosaic texture of the crystal J phase of compound **16** obtained at 118 °C on cooling.

methods.¹⁴ However, one unresolved aspect was the fact that the DSC showed a transition at 172 °C ($\Delta H = 1.8 \text{ kJ mol}^{-1}$) which did not correspond to a significant change in texture. At the present time we can offer no explanation for this, but in due course we plan to have the compound examined by X-ray methods in order to pin this behaviour down.

The broad pattern of mesomorphism in these ligands is rather similar to that of related monoimines which we have synthesized previously when studying related monometallic complexes.¹⁴

Mesomorphism of the complexes

The mesomorphism of the complexes is simply dealt with as it was non-existent! In each case the complexes melted directly to the isotropic phase (Table 3), occasionally with decomposition and in one case (**27**) passing through a second crystal modification. Having found this to be the case for dinuclear complexes of the four-ring imines, **15–20**, we wished to push the study one step further by synthesizing a dinuclear complex of a five-ring diimine (**21**) whose mesomorphism is reported above. In this case too the dinuclear complex proved to be non-mesomorphic, simply melting at 220 °C. Thus, it is absolutely clear that the introduction of the second $\text{Re}(\text{CO})_4$ unit destroys mesomorphism. It is, however, interesting to speculate a little on why this might be.

In the present study the ligands show predominantly smectic C and nematic phases extending up to, and above, 300 °C. In our previous studies similar ligands displayed a similar mesomorphism in a similar temperature range. In these previous studies, complexation of the ligands led to materials which showed only a nematic phase which formed from the crystal phase at somewhere between 130–150 °C and persisted until near 200 °C. In the present case two factors are apparent. First, in complexes **22–24**, the chain length has relatively little effect on the melting point which in any case is rather high at about 200 °C or above. The same situation is found for the dinuclear complex of the five-ring imine (**28**). In these cases, it might be postulated that the crystal phase is stabilised well above the temperature at which any mesophase might exist. It is impossible to show this for **22**, **23** and **28** which decompose on melting, but careful studies of **24** show that there is no evidence of a supercooled (monotropic) nematic phase below the crystal phase. Curiously, however, for **25–27** there is a much stronger dependence of the melting point on chain length, decreasing by 90 °C from butyloxy to dodecyloxy terminal chains. Once again, we find no evidence of any monotropic phases only this time, with melting points as low as 148 °C for **27**, we might reasonably have expected to see some evidence of a monotropic phase *unless* our strategy has been so successful that the transition temperatures are very much reduced. It is, of course, tempting to speculate that this might be the case but of course

Table 4 Microanalytical data (%) for the new ligands and complexes

		Calculated (Found)		
Compound	Yield	C	H	N
Diimines				
15	73	76.6 (76.4)	6.6 (6.5)	5.1 (5.1)
16	79	78.2 (78.4)	7.9 (8.0)	4.2 (4.2)
17	55	79.2 (79.3)	8.9 (8.9)	3.6 (3.6)
18	83	76.6 (76.5)	6.6 (6.5)	5.1 (4.9)
19	99	78.2 (78.2)	7.9 (7.9)	4.2 (4.0)
20	78	79.2 (79.1)	8.9 (8.9)	3.6 (3.5)
21	54	76.9 (77.0)	7.2 (7.2)	3.5 (3.5)
Dirhenium complexes				
22	38	45.1 (44.6)	3.0 (2.9)	2.4 (2.3)
23	42	48.8 (48.9)	4.0 (3.9)	2.2 (2.2)
24	17	51.8 (51.6)	4.9 (4.8)	2.0 (2.0)
25	65	45.1 (44.9)	3.0 (2.9)	2.4 (2.3)
26	64	48.8 (48.4)	4.0 (3.9)	2.2 (2.2)
27	74	51.8 (51.4)	4.9 (4.7)	2.0 (2.0)
28	51	50.6 (50.8)	3.9 (3.9)	2.0 (2.0)

there is no evidence whatsoever for such an argument at this time.

Experimental

Elemental analysis was determined by the University of Exeter Microanalysis Service. NMR spectra were recorded on either a Bruker ACF-300 or DRX-400 spectrometer, where the chemical shifts are reported relative to the internal standard of the deuteriated solvent used. Analysis by DSC was carried out on a Perkin-Elmer DSC7 instrument using heating and cooling rates of either 5 or 10 K min⁻¹. Analysis by hot stage microscopy was carried out using an Olympus BH40 microscope equipped with a Link-Am HFS91 hot stage, TMS92 controller and LNP2 cooling unit. Solvents were purified by standard methods before use. 4-Heptylbenzoic acid, 4-hexyloxyaniline and 4-heptyl-aniline were obtained from Aldrich. Yields and analytical data for new compounds are collected in Table 4.

Cell dimensions and intensity data for compounds **15**, **22** and **26** were recorded at 150 K, using an Enraf-Nonius KappaCCD area detector diffractometer mounted at the window of a rotating anode operating at 50 kV, 50 mA with a molybdenum anode ($\lambda(\text{Mo-K}\alpha) = 0.71073 \text{ \AA}$). The crystal-to-detector distance was 30 mm and ϕ and ω scans (2° increments, 10 s exposure time) were carried out to fill the Ewald sphere. Data collection and processing were carried out using the programs COLLECT,¹⁵ DENZO¹⁶ and MAXUS¹⁷ and an empirical absorption correction was applied using SORTAV.^{18,19} All structures were solved *via* direct methods²⁰ and refined by full matrix least squares²⁰ on F^2 . Non-hydrogen atoms were refined anisotropically and hydrogen atoms were placed in geometrical positions and refined using a riding model.

CCDC reference number 186/1902.

See <http://www.rsc.org/suppdata/dt/a9/a910273f/> for crystallographic files in .cif format.

Preparations

4-Octyloxybenzaldehyde, 2. 4-Hydroxybenzaldehyde (2 g, 16.4 mmol) was dissolved in butanone (100 cm³) and potassium carbonate (9 g, 65.6 mmol) and potassium iodide (0.2 g) added. 1-Bromooctane (4.8 g, 19.7 mmol) was added and the mixture heated at reflux under nitrogen for 48 h. On cooling, water (500 cm³) was added and the organic layer extracted with CH_2Cl_2 ($2 \times 150 \text{ cm}^3$). The combined organic extracts were washed with 5% aqueous NaOH ($2 \times 100 \text{ cm}^3$), dried over anhydrous Na_2SO_4 , filtered and evaporated to give a yellow oil. The crude product was purified by column chromatography (SiO_2 , eluent

CH_2Cl_2) and the solvent evaporated to give the pure yellow oil. Yield: 3.45 g (90%). ^1H NMR (400 MHz, CDCl_3): δ 0.90 (d, 3, CH_3), 1.45 (m, 10, 5 CH_2), 1.75 (m, 2, $\text{CH}_2\text{CH}_2\text{O}$), 4.0 (t, 2, $^3J_{\text{HH}} = 9.1$, CH_2O), 7.0 (AA'XX', 2, $J = 9$), 7.85 (AA'XX', 2, $J = 9$ Hz) and 9.9 (s, 1, CHO).

4-Butyloxybenzaldehyde **1** and 4-dodecyloxybenzaldehyde **3** were similarly prepared in yields of 83 and 88%, respectively.

4-Octyloxyaniline, 5. A solution of 1-bromooctane (7.03 g, 36.37 mmol) was added to a suspension of 4-acetamidophenol (5 g, 33.07 mmol) and potassium carbonate (9.2 g, 66.14 mmol) in butanone (80 cm^3). The mixture was heated at reflux for 18 h. After cooling, the solution was filtered through a Celite plug and the solvent evaporated. The residue was washed with Et_2O . After evaporation of the solvent a colourless powder was obtained. The filtrate was washed with a solution of NaOH ($2 \times 100 \text{ cm}^3$, 2 mol dm^{-3}), then NaCl ($2 \times 100 \text{ cm}^3$, 2 mol dm^{-3}), dried over Na_2SO_4 and the solvent again removed. The product was crystallised from hot ethanol (absolute) and a white solid obtained. The solid was dissolved in ethanol (100 cm^3 , 95%) and HCl (53.6 cm^3 , 35%) added. The solution was heated at reflux for 3 h. After filtration the solid was added to water (50 cm^3) and a solution of NaOH (2 mol dm^{-3}) added until pH 12. The solid was filtered off, dried and stored under N_2 at sub-ambient temperatures. Yield 4.95 g (56%). ^1H NMR (300 MHz, CDCl_3): δ 0.90 (t, 3, CH_3), 1.30 (m, 10, 5 CH_2), 1.80 (m, 2, $\text{CH}_2\text{CH}_2\text{O}$), 2.90 (br s, 2, NH_2), 4.40 (t, 2, CH_2O , $J = 6.8$), 6.55 (AA'XX', 2, $J = 8.8$) and 6.70 (AA'XX', 2, $J = 8.8$ Hz).

4-Dodecyloxyaniline **6** was similarly prepared in a yield of 60%, while 4-butyloxyaniline **4** was purchased from Aldrich.

4-[4-Octyloxybenzylideneamino]benzoic acid, 8. To a suspension of 4-octyloxybenzaldehyde **2** (0.5 g, 2.1 mmol) and 4-aminobenzoic acid (0.3 g, 2.1 mmol) in ethanol (40 cm^3 , absolute) were added a few drops of acetic acid (glacial). The mixture was heated at reflux for 15 min and then cooled to room temperature. The solid was filtered off crystallised from hot ethanol (absolute) and dried to yield a pure, off-white solid. Yield 0.6 g (81%). Found: C, 74.8; H, 7.7; N, 4.2. Calc. for $\text{C}_{22}\text{H}_{27}\text{NO}_3$: C, 74.8; H, 7.7; N, 4.0%. ^1H NMR (400 MHz, CDCl_3): δ 0.90 (t, 3, CH_3), 1.34 (m, 10, 5 CH_2), 1.81 (m, 2, $\text{CH}_2\text{CH}_2\text{O}$), 4.03 (t, 2, $^3J_{\text{HH}} = 6.4$, CH_2O), 7.0 (AA'XX', 2, $J = 8.8$), 7.21 (AA'XX', 2, $J = 8.8$), 7.83 (AA'XX', 2, $J = 8.8$), 8.12 (AA'XX', 2, $J = 8.8$ Hz), 8.12 (s, 1, $\text{CH}=\text{N}$) and 9.88 (s, 1, CO_2H).

4-[4-Butyloxybenzylideneamino]benzoic acid **7**, 4-[4-dodecyloxybenzylideneamino]benzoic acid **9**, 4-[4-butyloxybenzylideneamino]phenol **10**, 4-[4-octyloxybenzylideneamino]phenol **11** and 4-[4-dodecyloxybenzylideneamino]phenol **12** were similarly prepared in yields 70, 78, 83, 83 and 82% respectively.

4-Aminophenyl 4-aminobenzoate, 13. To a suspension of 4-nitrophenol (0.83 g, 3.5.98 mmol) was added to a suspension of 4-nitrobenzoic acid (1 g, 5.98 mmol), DCC (1 g, 7.17 mmol) and DMAP (17 mg) in CH_2Cl_2 (60 cm^3). The mixture was stirred under nitrogen for 18 h. The precipitate was filtered off and the solvent evaporated to give a yellow compound. The yellow crude product was purified by column chromatography (SiO_2 , eluent CH_2Cl_2) and the solvent evaporated to give a pure pale yellow powder. The powder was dissolved in THF (30 cm^3) and palladium on carbon (10 mg, 10%) was added. The mixture was kept under H_2 pressure (20 psi) overnight. The solution was filtered on a Celite plug and the solvent removed. The solid was crystallised from ethanol/hexane. Yield 0.91 g (67%). ^1H NMR (300 MHz, CDCl_3): δ 4.1 (s, 4, NH_2), 6.67 (2 overlapping AA'XX', 4, each $J = 7.9$), 7.0 (AA'XX', 2, $J = 7.9$) and 8.0 (AA'XX', 2, $J = 7.9$ Hz).

4-Formylphenyl 4-formylbenzoate, 14. To a suspension of 4-hydroxybenzaldehyde (1 g, 8.2 mmol) and 4-formylbenzoic

acid (1.23 g, 8.2 mmol) in CH_2Cl_2 (60 cm^3) was added DCC (2.03 g, 9.84 mmol) and DMAP (24 mg). The mixture was stirred under nitrogen for 18 h. The precipitate was filtered off and the solvent evaporated to give a yellow compound. The yellow crude product was purified by column chromatography (SiO_2 , eluent CH_2Cl_2) and the solvent evaporated to give a pure pale yellow powder. Yield 1.36 g (65%). Found: C, 70.8; H, 3.9. Calc. for $\text{C}_{15}\text{H}_8\text{O}_4$: C, 70.8; H, 4.0%. ^1H NMR (300 MHz, CDCl_3): δ 7.45 (AA'XX', 2, $J = 7.9$), 8.05 (AA'XX', 2, $J = 7.9$), 8.10 (AA'XX', 2, $J = 7.9$), 8.45 (AA'XX', 2, $J = 7.9$ Hz), 10.0 (s, 1, CHO) and 10.2 (s, 1, CHO).

Diimine 16. To a suspension of 4-[4-octyloxybenzylideneamino]benzoic acid **8** (1.08 g, 3.07 mmol) and 4-[4-octyloxybenzylideneamino]phenol **11** (1.0 g, 3.07 mmol) in CH_2Cl_2 (100 cm^3) were added DCC (0.76 g, 3.68 mmol) and DMAP (9 mg). The mixture was stirred under nitrogen for 18 h. The precipitate was filtered off and the solvent evaporated to give a yellow powder. The solid was crystallised from CH_2Cl_2 /hexane. Yield 1.60 g (79%). ^1H NMR (400 MHz, CH_2Cl_2): δ 0.90 (t, 6, CH_3), 1.33 (m, 16, 8 CH_2), 1.48 (m, 2, 8 CH_2), 1.82 (m, 4, $\text{CH}_2\text{CH}_2\text{O}$), 4.03 (m, 4, 2 CH_2O), 6.98 (2 AA'XX', 4), 7.26 (3 AA'XX', 6), 7.85 (2 AA'XX', 4), 8.23 (AA'XX', 2), 8.38 (s, 1, $\text{CH}=\text{N}$) and 8.40 (s, 1, $\text{CH}=\text{N}$). Diimine **15** was similarly prepared.

Diimine 17. To a suspension of 4-dodecylbenzaldehyde **3** (0.73 g, 2.49 mmol) and 4-aminophenyl 4-aminobenzoate **13** (0.19 g, 0.83 mmol) in ethanol (40 cm^3 , absolute) were added a few drops of acetic acid (glacial). The mixture was stirred overnight at room temperature. The resulting solid was filtered off, crystallised from CH_2Cl_2 /hexane and dried to yield a pure off-white solid. Yield 0.35 g (55%). ^1H NMR (300 MHz, CDCl_3): δ 0.90 (t, 6, CH_3), 1.30 (m, 32, 8 CH_2), 1.50 (m, 4, 8 CH_2), 1.90 (m, 4, $\text{CH}_2\text{CH}_2\text{O}$), 4.03 (m, 4, CH_2O), 6.98 (AA'XX', 2, $J = 8.4$), 6.99 (AA'XX', 2, $J = 8.4$), 7.25 (3 overlapping AA'XX', 6), 7.90 (2 overlapping AA'XX', 4, each $J = 8.4$), 8.20 (AA'XX', 2, $J = 8.4$ Hz), 8.38 (s, 1, $\text{CH}=\text{N}$) and 8.40 (s, 1, $\text{CH}=\text{N}$).

Diimine 19. To a suspension of 4-octyloxyaniline **5** (0.57, 2.59 mmol) and 4-formylphenyl 4-formylbenzoate **14** (0.3 g, 1.18 mmol) in ethanol (40 cm^3 , absolute) were added a few drops of acetic acid (glacial). The mixture was stirred overnight at room temperature. The resulting solid was filtered off, washed with hot ethanol (absolute) and dried to yield a pure off-white solid. Yield 0.77 g (99%). ^1H NMR (400 MHz, CH_2Cl_2): δ 0.91 (t, 6, CH_3), 1.32 (m, 16, 8 CH_2), 1.49 (m, 2, 8 CH_2), 1.81 (m, 4, $\text{CH}_2\text{CH}_2\text{O}$), 4.00 (m, 4, CH_2O), 6.95 (AA'XX', 2, $J = 8.8$), 6.96 (AA'XX', 2, $J = 8.8$), 7.26 (AA'XX', 2, $J = 8.8$), 7.32 (AA'XX', 2, $J = 8.8$), 7.38 (AA'XX', 2, $J = 8.8$), 8.01 (AA'XX', 2, $J = 8.8$), 8.08 (AA'XX', 2, $J = 8.8$), 8.31 (AA'XX', 2, $J = 8.4$ Hz), 8.54 (s, 1, $\text{CH}=\text{N}$) and 8.63 (s, 1, $\text{CH}=\text{N}$).

Diimines **18**, **20** and **21** were similarly prepared.

Complex 23. To a suspension of diimine **16** (55 mg, 0.076 mmol) in toluene (20 cm^3) was added pentacarbonylmethylrhenium(i) (57 mg, 0.167 mmol). The reaction mixture was stirred under reflux for 20 hours, under a nitrogen atmosphere and then cooled to room temperature and the solvent removed. The yellow solid was dissolved in CH_2Cl_2 and purified by column chromatography on alumina with CH_2Cl_2 as eluent. The solution was concentrated and hexane added to give the pure yellow solid in 42% yield (40 mg). ^1H NMR (400 MHz, CD_2Cl_2): δ 0.92 (2 t, 6, 2 CH_3), 1.35 (m, 16, CH_2), 1.50 (m, 4, CH_2), 1.84 (m, 4, 2 $\text{CH}_2\text{CH}_2\text{O}$), 4.11 (2 t, 4, 2 CH_2O), 6.72 (2dd, 2, $^3J_{\text{HH}} = 8.0$, $^4J_{\text{HH}} = 4.0$, 2 H_b), 7.36 (2 AA'XX', 4, $J = 8.4$), 7.39 (AA'XX', 2, $J = 8.4$), 7.44 (AA'XX', 2, $J = 8.8$), 7.54 (d, 1, $^4J_{\text{HH}} = 4$, H_a), 7.57 (d, 1, $^4J_{\text{HH}} = 4$, H_a), 7.69 (d, 1, $^3J_{\text{HH}} = 8.4$, H_c), 7.73 (d, 1, $^3J_{\text{HH}} = 8.4$, H_c), 8.32 (AA'XX', 2, $J = 8.8$ Hz), 8.50 (s, 1, $\text{CH}=\text{N}$) and 8.5 (s, 1, $\text{CH}=\text{N}$).

All other dirhenium complexes (**23**, **24–28**) were prepared in the same way.

Acknowledgements

We would like to thank H. C. Stark for a generous gift of rhenium, the EU for a Marie Curie Fellowship (to M. A. G.) and Professor John Goodby of the University of Hull for help with the microscopy of ligand **21**.

References

- 1 D. W. Bruce and D. O'Hare, *Inorganic Materials*, 1996, Wiley, Chichester, 2nd edn., 1996.
- 2 B. Donnio and D. W. Bruce, *Struct. Bonding*, (Berlin), 1999, **95**, 193.
- 3 D. W. Bruce, *Adv. Mater.*, 1994, **6**, 699.
- 4 D. W. Bruce and X.-H. Liu, *J. Chem. Soc., Chem. Commun.*, 1994, 729.
- 5 X.-H. Liu, M. N. Abser and D. W. Bruce, *J. Organomet. Chem.*, 1998, **551**, 271.
- 6 D. W. Bruce and X.-H. Liu, *Liq. Cryst.*, 1995, **18**, 165.
- 7 M.-A. Guillevis, M. J. Danks, S. K. Harries, S. R. Collinson, A. D. Pidwell and D. W. Bruce, *Polyhedron*, 2000, **19**, 249.
- 8 S. Morrone, D. Guillon and D. W. Bruce, *Inorg. Chem.*, 1996, **35**, 7041.
- 9 K. E. Rowe and D. W. Bruce, *J. Chem. Soc., Dalton Trans.*, 1996, 3913.
- 10 N. Miyajima and Y. Matsunaga, *Mol. Cryst., Liq. Cryst.*, 1995, **260**, 499.
- 11 W. Beck and K. Raab, *Inorg. Synth.*, 1990, **28**, 15.
- 12 V. N. Kalinin, V. I. Zdanovich, P. V. Petrovskii, A. S. Batsanov and Yu. T. Struchkov, *Metalloorg. Khim.*, 1990, **3**, 662.
- 13 G. W. Gray and J. W. Goodby, *Smectic Liquid Crystals: Textures and Structures*, Leonard Hill, Glasgow, 1984.
- 14 X.-H. Liu, B. Heinrich, I. Manners, D. Guillon and D. W. Bruce, *J. Mater. Chem.*, 2000, **10**, 637.
- 15 COLLECT data collection software, Nonius B.V., Delft, 1998.
- 16 Z. Otwinowski and W. Minor, *Methods Enzymol.*, 1997, **276A**, 307.
- 17 S. Mackay, C. J. Gilmore, C. Edwards, M. Tremayne, N. Stuart and K. Shankland, MAXUS, a computer program for the solution and refinement of crystal structures from diffraction data, University of Glasgow, Nonius BV, Delft, and MacScience Co. Ltd., Yokohama, 1998.
- 18 R. H. Blessing, *Acta Crystallogr., Sect. A*, 1995, **A51**, 33.
- 19 R. H. Blessing, *J. Appl. Crystallogr.*, 1997, **30**, 421.
- 20 SHELX 97: Programs for Crystal Structure Analysis (Release 97–2), G. M. Sheldrick, University of Göttingen, 1998.